Numerical Methods in Civil Engineering, 9-1 (2024) 30-41

Numerical Methods in Civil Engineering

Journal Homepage: https://nmce.kntu.ac.ir/

Analysis of the Numerical Results Obtained from the Experimental Examination of the Mechanical Properties of Geopolymer Concrete

Mohammadhossein Mansourghanaei*, Alireza Mardookhpour**

ARTICLE INFO

RESEARCH PAPER

Article history:
Received:
February 2024
Revised:
May 2024
Accepted:
August 2024

Keywords:
Geopolymer Concrete,
Blast Furnace Slag,
Nano-Silica,;
Polyolefin Fibers,
High Temperature

Abstract:

Activated alkaline slag concretes (AASC), also known as geopolymer concretes (GPCs), are concretes with high mechanical properties. Theoretical alkali-active materials, granulated blast furnace slag (GBFS) and nano-silica (NS) contain aluminosilicate materials that play an effective role in improving the mechanical properties of concrete. The use of fibers such as polyolefin fibers (POFs). in the composition of concrete improves the resistance of concrete against applied loads. In this research, tests of compressive strength, tensile strength, modulus of elasticity, impact of falling weight, and determining the ultrasonic pulse velocity (UPV), scanning electron microscope (SEM), X-Ray fluorescence (XRF) and X-Ray diffraction (XRD), at the age of 90 days under 25 and 500 °C was done on GPCsThe results demonstrate that adding NS to GPCs changes the resistance of the sample against heating treatment in the compressive strength test from 16.4 to 8.4%, from 21 to 13% in the tensile strength test, and 41 to 33% in the modulus of elasticity. Besides, the presence of POFs in the GPCs mixture substantially affect tensile strength, and resistance against an impact. In the following, the results UPV test are compared and evaluated through numerical investigations by conducting UPV tests and analysis SEM, XRD and XRF.

1. Introduction

GBFS is considered an environmentally friendly material. Using this material instead of cement can improve concrete resistance and decrease the growing demand for its usage in concrete [1, 2]. Comparing the concrete containing regular Portland cement with GPCs [3], McNulty [4], asserted that the GPCs have higher compressive strength [5]. Several studies have shown that GPCsS exposed to high temperatures have better performance than ordinary portland cement concrete (OPCC). [6-8].

The resistance of GPCs under high temperature depends on several factors such as the amount of heat, curing, and chemical composition [9]. Kong et al. [10] investigated the behavior of GPCs at a high temperature, depending on the size of the aggregates. They realized that the resistance loss in GPCs samples at a higher temperature was probably due to the thermal inconsistency between the geopolymer matrix and the entire mixture's constituents. The bonding types the constituent components of concrete and the characteristics of each component in OPCC and GPCs are different from each other [11-13]. In addition to positively affecting the mechanical properties, the presence of silica particles in the GPCs accelerates the geopolymer reaction and reduces the compound alkalinity [14]. Such being a case mitigates the drawbacks of the utilized fiber. According to the investigations, NS addition to the GPCs enhances its compressive strength until the Silica to Aluminum (Si/Al) ratio reaches 2% in the mixture and further silica addition decreases the compressive strength due to agglomeration and non-uniform distribution [15]. An improvement was reported in the respective compressive strength [16], modulus of elasticity, and ultrasonic wave velocity using NS particles in the GPCs compound [17]. In another study on the GPCs cured at an ambient temperature, the effect of 0-10% NS addition to the samples was investigated in different concentrations of sodium hydroxide (NaOH) activator liquid (8, 10, 12 M). Accordingly, the compressive and tensile

*Corresponding Author: Ph.D. in Civil, Department of Civil Engineering, Chalous Branch, Islamic Azad University, Chalous, Iran.
*E-Mail Address:*Mhm.Ghanaei@Gmail.com
**Department of Civil Engineering, Lahijan Branch, Islamic Azad University, Lahijan, Iran. E-Mail Address: Ar.Mardookhpour@Gmail.com

https://doi.org/1061186/NMCE.2402.1047

strength improvement and optimal water absorption coefficient were obtained in 6% NS addition [18]. Research has shown that the use of POFs fibers in concrete composition is effective in preventing crack propagation under applied loads and improving mechanical properties [19-24]. By performing Crack Mouth Opening Displacement (CMOD) analysis, it is revealed that the POFs have favorable bonding properties. Moreover, due to its proper stiffness after the initial crack creation, it holds the concrete parts together [25]. In an investigation conducted on the effect of adding 0.5 of POFs to the alkali activated slag concretes, it is observed that the compressive strength of the samples declined by 12-15%. The samples containing fibers with 55 mm in length had undergone lower compressive strength more than those with 48 mm in length [26]. This study mainly aims to investigate the mechanical properties of the alkali activated slag concretes based on the slag containing NS and also reinforced with POFs. For this purpose, the compressive and tensile strength, modulus of elasticity, and impact tests have been conducted. To accurately analyze the ultrasonic wave velocity test and also the relationship between the compressive strength and modulus of elasticity, the compressive strength, and ultrasonic wave velocity have also been examined. Ultimately, the microstructure caused by samples' exposure to the heating treatment is examined by SEM and XRD tests.

2. Experimental

2.1 Materials

In this article, materials with these characteristics were used in the combination of OPCC and GPC, type 2 concrete with a density of 2350 kg/m^3, GBFS produced by Isfahan factory with a density of 2450 kg/m^3 with chemical properties according to Table 1, aggregates They were under the ASTM C33 standard. The NS particles with 99.5 SiO_2, an average diameter of 7-14 nm, and a specific weight of 0.7 g/cm^3 have been used in this investigation. Furthermore, the corrugated POFs has been used with 30 mm in length, 0.8 mm in diameter, and 0.72 g/cm^3 of specific weight according to ASTM D7508/D7508M standard.

Table 1: Chemical Properties of Materials (%)

Component	SiO_2	Al_2O_3	Fe_2O_3	CaO	MgO	SO_3	K_2O	Na_2O	TiO_2	LOI
GBFS	29.2	19.4	5.8	38.6	2.8	2.6	0.1	0.2	0.6	0.3
Portland Cement	21.3	4.7	4.3	62.7	2.1	2	0.65	0.18	-	1.84

Table 2: Mix Design (Kg/m^3)

	Mix Design	OPC	GBFS	Water	AAS	NS	CA[1]	FA[2]	POFs	SP
1	OPCC	450	0	202.5	0	0	1000	761.13	0	9
2	GPCNS0POF0	0	450	0	202.5	0	1000	816.10	0	9
3	GPCNS4POF0	0	432	0	202.5	18	1000	767.42	0	10
4	GPCNS8POF0	0	414	0	202.5	36	1000	718.75	0	11
5	GPCNS8POF1	0	432	0	202.5	36	1000	672.78	24	11
6	GPCNS8POF2	0	432	0	202.5	36	1000	646.28	48	11

2.2 Mix Design

The mixing design in this laboratory research was set according to the standard ACI 211.1-89 as described in Table 2. In this regard, design 1 includes OPCC, design 2 includes GPC containing 100% GBFS, design 3 includes GPC containing 96% GBFS and 4% NS, design 4 includes GPC containing 92% GBFS and 8% NS, design 5 includes GPC containing 92% GBFS, 8% NS, 1% POFs and design 6 includes GPC containing 92% GBFS, 8% NS, 2% POFs. Designs 5 and 6 include adding 1 and 2 percent POFs to design 4, which is optimal for designs 2 to 4. Active alkali solution (AAS) of the type NaOH and Na_2SiO_3 with a molarity of 12 is used instead of water in the composition of GPC (schemes 2 to 6). Investigations by other researchers have shown that the combined use of NaOH and Na_2SiO_3 in the composition of GPC increases the mechanical properties of concrete [27].

2.3 Experimental Program and Standards

In this laboratory research, 180 concrete samples (90 samples at ambient temperature and 90 samples at high temperature) were considered for tests. After molding the samples, the samples were placed under the temperature of

[1] Coarse Aggregates (CA)
[2] Fine Aggregates (FA)

80 °C for 48 hours and then stored in a dry environment for 90 days. In the high temperature tests, the samples were kept in the furnace at a temperature of 500 °C for 1 hour. In the following and before performing each test under high heat, the samples reached the ambient temperature [10]. In this research, the compressive strength test was performed on 10 cm cubic samples under BS EN 12390 [29] standard. Tensile strength test was performed on 15×30 cm cylindrical samples under ASTM C496 standard [30]. The UPV test was performed under the ASTM C597 [31] standard on 10 cm cubic samples. The drop weight impact test under the ACI 544-2R [32] standard was performed on 15×6.35 cm disc samples. SEM analysis under ASTM C1723 standard, XRD analysis under BS EN13925 standard and XRF analysis under ASTM E1621 standard were performed.

3. Results and Discussion

3.1 The Results of Compressive Strength Test

High temperature can have a direct effect on the microstructure and macrostructure of concrete. High heat leads to weakening of bonds in Interfacial Transition Zone (ITZ) concrete. On the other hand, high heat damages the chemical structure of the materials in the concrete composition.

Research has shown that high temperatures can cause significant changes to geopolymer concrete, including [33]:

1. Evaporation of water required in the process of geopolymerization of GPC at 100 °C.
2. The process of geopolymerization of GPC starts at a temperature of 180 °C.
3. Increase in volume of vapor pressure in GPC composition at 200 °C.
4. The beginning of the dihydroxylation process at a temperature of 500 °C.
5. Creation of a porous ceramic structure in the concrete mixture at a temperature of 800 °C and a high drop in concrete strength.

Of course, the reduction of strength in concrete in the range of 500 °C heat application begins with changes in the structure of the gel C-S-H [34,35].

In this research, the results of the compressive strength test are shown in the diagram of Figure 1. The results indicate that the compressive strength of GPC is superior to that of OPCC under temperatures of 25 and 500 °C. The results indicate that high temperature has led to a drop in the compressive strength of OPCC (up to 37%) and GPC (up to 16%). The strength loss of GPC containing NS under high heat (up to 11%) is less than that of GPC without NS due to the higher percentage of bonding in ITZ due to the production of larger volume of hydrated gels.

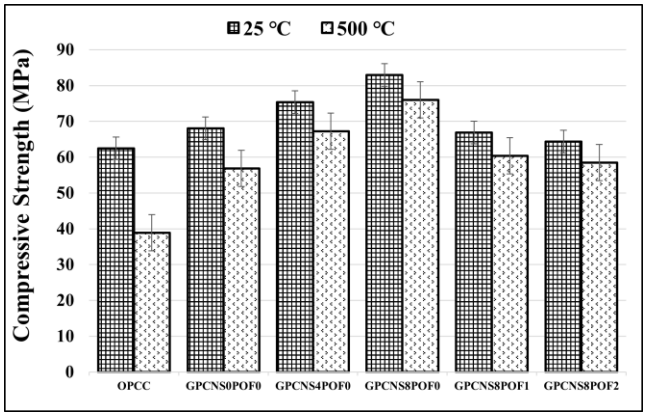

Fig. 1: Compressive Strength Test Results

3.2 The Results of Tensile Strength Test

The results of the tensile strength test under the temperature of 25 and 500 °C are shown in the graph of Figure 2. Based on these results, it can be seen that the tensile strength of GPC containing POFs under the temperature of 25 (up to 25%) and 500 (up to 90%) degrees is higher than GPC without POFs and OPCC at the corresponding temperature. This superiority is due to the good resistance of the POFs between the cracked plates under tensile load. The increase in temperature from 25 to 500 **°C** has caused the tensile strength of OPCC to drop by 50% and GPC to 21%. The addition of NS to GPC, up to 25% at 25 **°C** and up to 36% at 500 **°C** has improved the tensile strength of GPC.

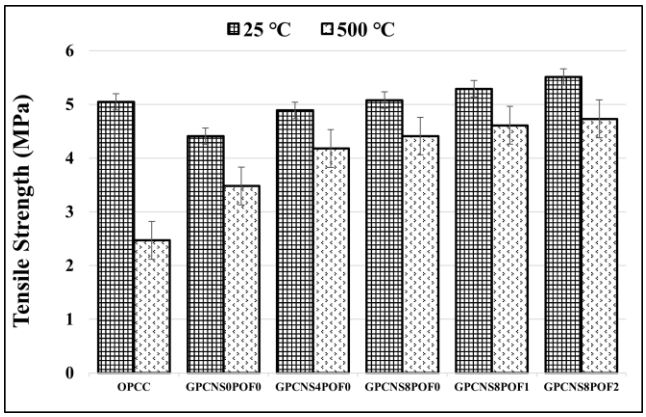

Fig. 2: Tensile Strength Test Results

3.3 The Relationship Between Tensile Strength and Compressive Strength Test Results

Table 3 demonstrates the relationship between compressive strength and tensile strength under different conditions applied by different researchers. In this regard, Eq (1) is obtained for regular concrete, and Eq (2) is obtained for GPCs cured at 60°C oven. Eq (3) is the relationship between strengths in GPCs cured at room temperature. Eq (4) is pertinent to the study on GPCs at room temperature in this article.

As indicated in Figure 3, the relationship achieved for concrete at 500°C is erroneous. Eq (1), attained for regular concrete, is very close to the obtained Eq(4) (for 90 days at room temperature), and the difference between these two is 12%. On the other hand, Eq (1) predicted greater values for tensile strength in concrete. Eq (2) is consistent with this research and has an error mean of 8%, and the predicted tensile strength predicted by this regulation is greater than the acquired results. Eq (3) is extremely different from the obtained Eq (5) due to curing at room temperature and has an error mean of 37%, indicating the importance of curing temperature. Eq (3) cannot be employed for GPCs cured at 60 °C.

Table 3: The Relationships Between the Compressive and Tensile Strength Test Results of Concrete

	Eq	Ref
1	$f_t = 0.59\sqrt{f_c}$	ACI363R-92 [36]
2	$f_t = 0.93(f_c)^{0.5}$	Nath [37]
3	$f_t = 0.69(f_c)^{0.5}$	Diaz [38]
4	$f_t = 0.2172(f_c)^{0.7158}$	The Equation in Ambient Temperature in This Study
5	$f_t = 0.1239(f_c)^{0.8287}$	The Equation in This Study Temperature of 500 °C

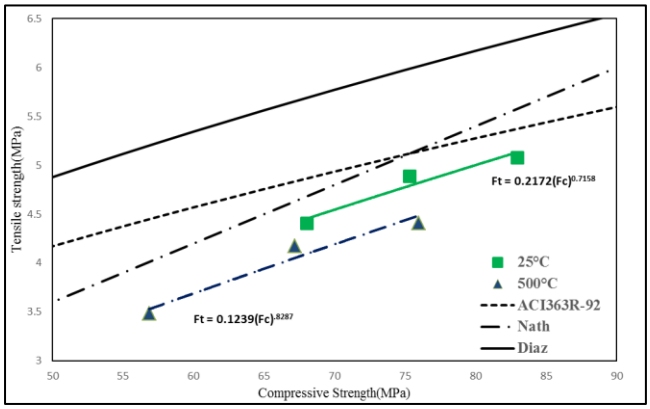

Fig. 3: Relationships Between the Compressive and Tensile Strength Test Results of Concrete

3.4 The Results of Elastic Modulus Test

In Figure 3, the elastic modulus diagram of concrete samples in the previous study is presented. According to this diagram, as heat increases in concrete samples, the elastic modulus decreases. This amount of decrease is 59% and 42% for regular concrete and alkali-activated slag concrete, respectively. By adding 4% and 8% NS to the GPC mixture, the reduction in elastic modulus in concrete under heating treatment decreased to 37% and 31%, respectively. The reduction level in elastic modulus in designs 5 and 6 is 31%.

The results achieved in Figure 4 imply that the improvement in elastic modulus due to the addition of 1% and 2% fibers in samples is 1.5 and 7%, respectively. With the addition of 4% and 8% NS, this amount increased to 12% and 13%, respectively, compared to the sample without NS. Using alkali activated slag instead of regular concrete increased elastic modulus by 8%. The addition of NS to concrete containing fibers leads to two cases: the first case is pertinent to concrete density. By adding NS, the concrete density increases and leads to an increase in the elastic modulus of concrete. The second case is pertinent to the filler feature of NS. As long as the pores of the concrete are not filled, increasing the amount of NS leads to an increase in elastic modulus. However, when the amount of NS increases excessively, the agglomeration phenomenon reduces the dynamic elastic modulus in concrete.

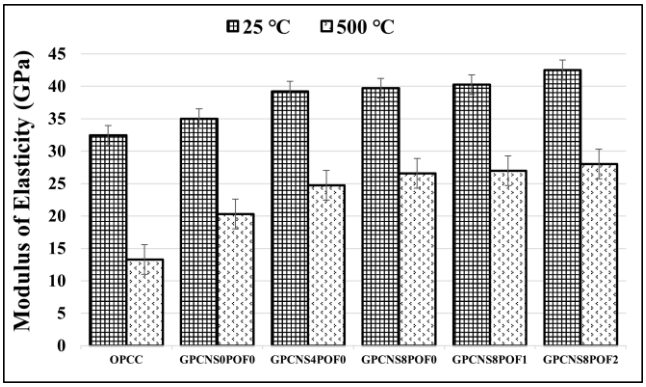

Fig. 4: The Results of the Modulus of Elasticity test

3.5 The Relationship Between Compressive Strength and Elastic Modulus Test Results

Figure 5 illustrates the variation in elastic modulus versus variation in compressive strength in this experimental study. The obtained results demonstrated in this Figure indicate that elastic modulus increases as compressive strength increases. Prediction of samples' elastic modulus concerning compressive strength gained in this research and using presented relationships are reported in Table 4. In this Table, Eq (6) is for regular concrete, and Eqs (7) and (8) are for alkali activated slag concrete, which is reported by two researchers. Despite being proposed for regular concrete, Eq (6) is consistent with the Equation proposed in this study, and its error mean is less than 7%. Eq (7) is for alkali activated slag concrete, and its error mean is 6% greater than that of the Equation in this research. Eq (8) is pertinent to GPC containing a low amount of calcium fly ash, which is cured at room temperature. In Eq (8), the error value compared to experimental results(Eqs (9) and (10)) is 28%, indicating the importance of curing temperature. In this research, the curing temperature is considered 60°C. Thus, Eq (7) in which the curing temperature is equal to room temperature cannot be employed.

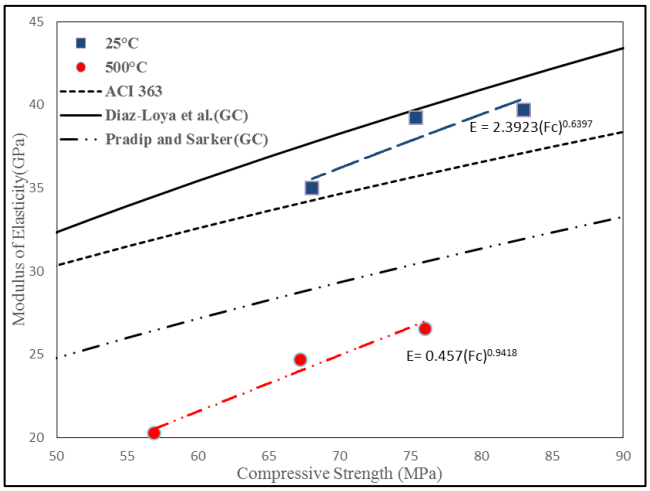

Fig. 5: Relationships Between the Compressive Strength and Elastic Modulus Test Results of Concrete

Table 4: The Relationships Between the Compressive Strength and Elasticity Modulus Test Results of Concrete in This Research and Other Researches

	Eq	Ref
6	$E_c = 3320\left(f'_c\right)^{0.5} + 6900$	ACI 363 [39]
7	$E_c = 0.037 \times \rho^{1.5} \left(f_c\right)^{0.5}$	Diaz-Loya et al.(GC) [40]
8	$E_c = 3510\left(f_c\right)^{0.5}$	Pradip and Sarker(GC) [37]
9	$E_c = 2392.3\left(f_c\right)^{0.6397}$	The Equation in Ambient Temperature in This Study
10	$E_c = 457\left(f_c\right)^{0.9418}$	The Equation in This Study Temperature of 500 °C

3.6 The Results of the UPV Test

The results of the UPV test are shown in the diagram of Figure 6 and the relationship between the results of the compressive strength test and the UPV test are shown in Figure 7. The results indicate the high speed of ultrasonic waves passing through OPCC and GPC at a temperature of 25 °C, so that all the samples are in excellent concrete quality according to the IS 13311-1 standard [31]. However, applying heat of 500 °C has led to a decrease in the speed of waves passing through concrete. This issue is mostly due to the change in concrete structure and weakening ITZ. So the quality of GPC has dropped to a good rank. The addition of 8% NS to the composition of GPC at a temperature of 25 °C to 11% and at a temperature of 500 °C to 14% has led to an increase in the speed of UPV in this type of concrete. The addition of POFs to the GPC composition has decreased the speed of UPV in this type of concrete. The addition of NS to the GPC composition has improved UPV by up to 40%. The addition of POFs to the GPC mix has resulted in a reduction of UPV, this is due to the reduction of POFs bonding in ITZ [41]. Research has shown that the high quality of concrete indicates the reduction of cracks in the concrete composition [42-44]. The exponential relationship between ultrasonic wave velocity and compressive strength for different alkali activated slag samples is shown in Figure 7.

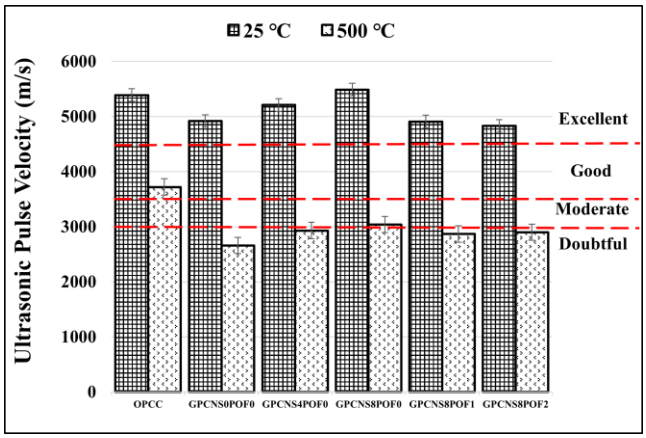

Fig. 6: UPV Results Test

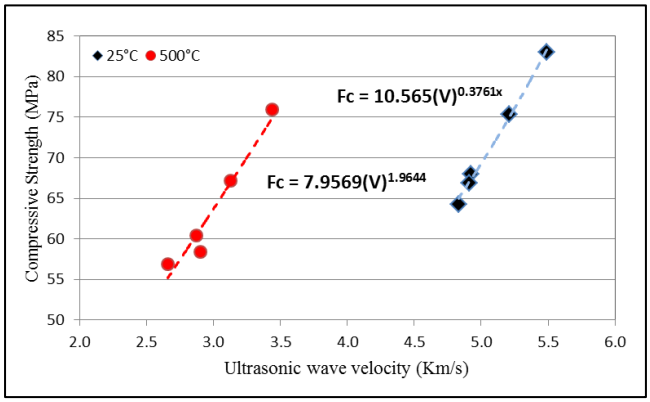

Fig. 7: Relationships Between the Compressive Strength and UPV Test Results of Concrete

3.7 The Results of the Impact Resistance Test

Impact energy is indicated in Figure 8, and absorbed energy and flexibility of concrete samples in this research are illustrated in Figure 9. Acquired results denote that increasing the temperature of concrete samples to 300°C insignificantly decreases impact energy until the initial crack is created. However, increasing the impact energy until thorough failure of samples is observed. Generally, an increase in resistance is witnessed between room temperature and 200 °C and even 300 °C in research by other researchers, and various reasons are attributed to this increase. For instance, Sadighi et al. in 2012 [4] attributed this increase to the quick drying of concrete. Similar reports are also provided [35,45].

Some others attributed this increase to the rehydration of paste due to the movement of water inside capillary cavities. As temperature increases, i.e., at 300 °C, it is realized that

the impact energy for the creation of initial crack and final spalling is extremely decreased for all samples.

According to the results found in this section, it is identified for all groups that as the percentage of POFs increases by 1% and 2% in alkali activated slag compound, the number of impacts for creation of initial crack and final spalling of samples increases. This means that the energy absorption capacity of GPCs increases with the addition of fibers. POF is significantly resistant to the creation and expansion of cracks during concrete structure spalling, leading to stress concentration mitigation on the crack tip, and delaying the damage process under impact loads.

Increasing loading leads to the development and expansion of cracks. Crack expands to the vicinity of fibers until separation appears in the fibers and matrix surface. Due to tensile stress that occurs on the predicted path of crack, the power (concentration) on the crack tip decreases after the crack reaches the surface of fibers and its path deviates. This condition prevents further expansion of the crack. This consequence describes bridging or capacity of limiting crack in a block of concrete reinforced by fibers. The process by which fibers prevent crack expansion by bridging is indicated in Figure 10 in the form of the spalling pattern of concrete samples. As can be seen in this Figure, there is no crack on separated parts in the samples lacking fibers. However, in the samples containing fibers, the separated parts have microcracks due to the bridging effect of POFs, preventing crack expansion and maintaining uniformity of concrete.

When comparing concrete containing and lacking nano-silica, few microcracks are observed at the time of spalling, causing an insignificant increase in impact resistance. On the other hand, the effectiveness of fibers when facing impact loads is much more than NS in concrete samples. Besides, by the addition of POFs to alkali activated slag concrete, concrete has become more flexible. This behavior is also observed by other fibers in the investigations conducted by other researchers[20, 46].

The results achieved in this investigation indicated that the effect of POFs on the impact resistance of GPCs is extremely higher than that of NS. In this regard, by adding 1% and 2% POFs to concrete samples, the impact energy for the creation of the initial crack increases by 13% and 30%, respectively. The impact energy against thorough rupture increased by 231% and 345%, respectively. As shown by the research outcomes, the addition of fibers is more effective in complete rupture than in the appearance of the initial crack. The flexibility index for the addition of 1% and 2% POFs to GPCs is obtained at 2.8% and 3.4%, respectively. The amount of absorbed energy due to the addition of 1% and 2% of fiber increased by 6.2 and 9.3 times, respectively, indicating the favorable performance of fibers in adsorption of impact energy. With the addition of 4% and 8% NS to alkali activated slag concrete, the energy for creating the initial crack experienced a 62% and 77% increase, respectively. It also a 46% and 58% increase the energy for thorough rupture of concrete samples. Compared to regular concrete, the energy required for the appearance of an initial crack and thorough rupture of the sample increased by 44% and 14% in alkali activated slag concrete, respectively.

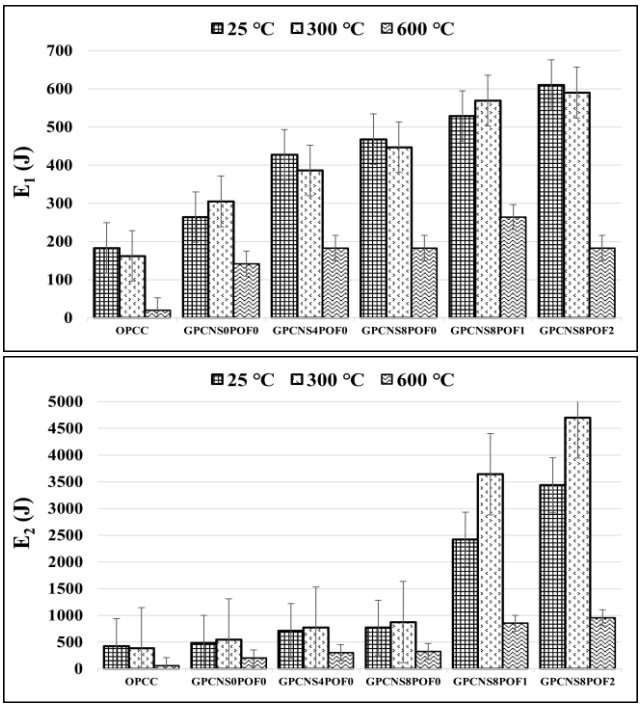

Fig. 8: Impact Energy Until the Creation of Initial Crack and Final Rupture of Samples

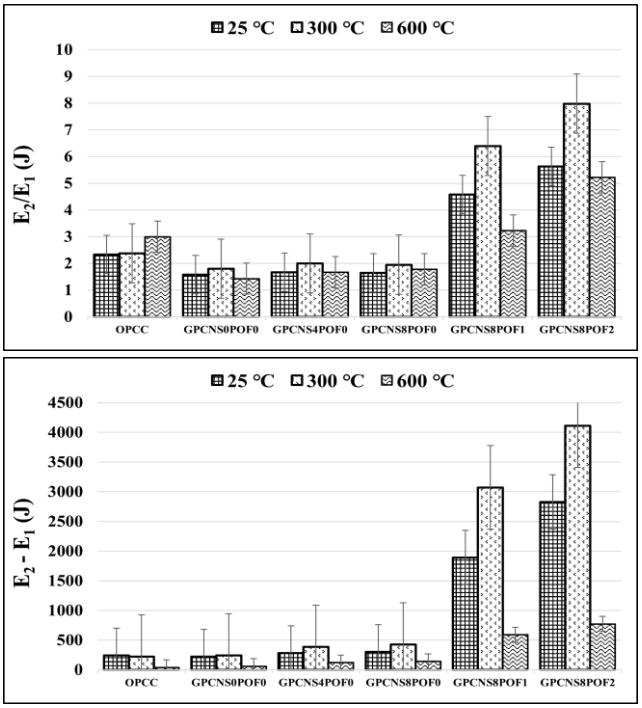

Fig. 9: The Percentage of Absorbed Energy of Different Samples and Flexibility

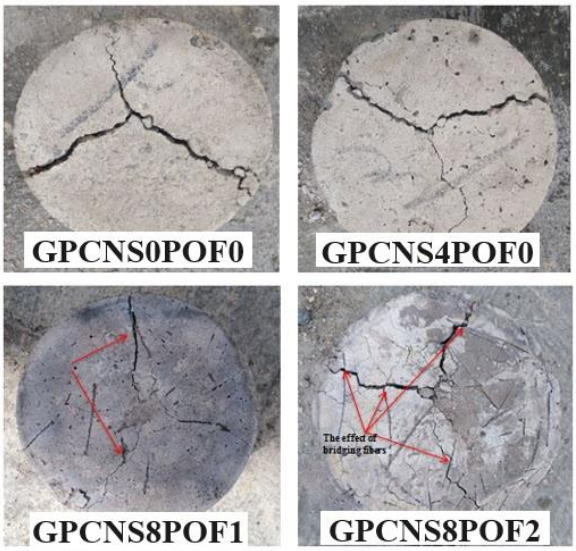

Fig. 10: Spalling Pattern of Samples with and Without POFs

3.8 Results of SEM Analysis

The results of SEM analysis of OPCC at temperatures of 25 and 500 °C are shown in Figure 11. The volume of hydrated gels (such as C-S-H) in the samples under ambient temperature is at a favorable level, but the temperature of 500 °C has led to an increase in the amount number of holes and cracks in the concrete sample. High heat disrupts the bonds in ITZ. The results of SEM analysis of GPGs at temperatures of 25 and 500 °C are shown in Figure 12. GPCs have a denser microstructure than OPCC, which is due to the production of a higher volume of hydrated gels such as C-S-H due to the aluminosilicate properties in its constituent materials [47,48]. In this regard, it can be seen in Figure 12 that the volume of hydrated gels produced in GPCs is more than OPCC, on the other hand, the amount of holes and microcracks in GPCs is less than OPCC. High temperature has changed the structure of GPCs. The results of SEM analysis of GPCNS8POF0 at temperatures of 25 and 500 °C are shown in Figure 13. The addition of NS up to 8% to the composition of GPC has improved the density of the matrix part of the concrete microstructure, this issue is evident in this figure. The gel containing small NS particles has reduced the holes and microcracks in the concrete composition. The density and quality of the microstructure of concrete in this design of GPC is higher than GPC without NS and 4% NS. The heat of 500 °C to this design of GPC has weakened the concrete structure in ITZ. The results of SEM analysis of GPCNS8POF1 at temperatures of 25 and 500 °C are shown in Figure 14. In this design, the bond areas between GPC paste and POFs (ITZ) are clearly defined. The heat of 500 °C has created a tree structure in this design of GPC. The tree structure includes holes, cracks, and bond discontinuity in ITZ. This type of structure will decrease the resistance of concrete against incoming loads.

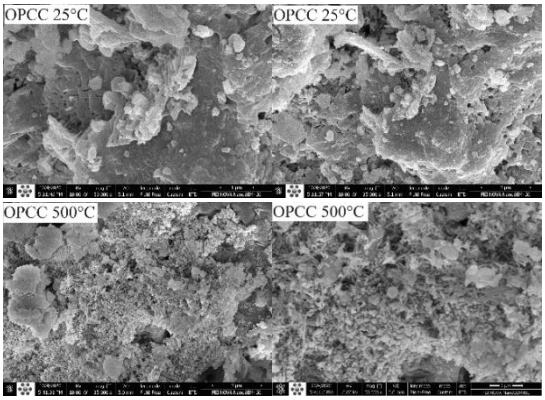

Fig. 11: SEM For the OPCC at 25 and 500 °C

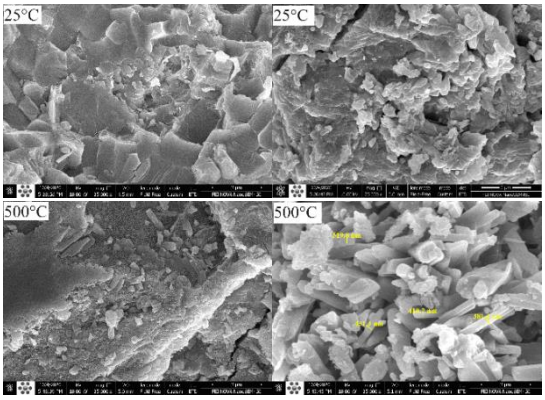

Fig. 12: SEM for the GPCs at 25 and 500 °C

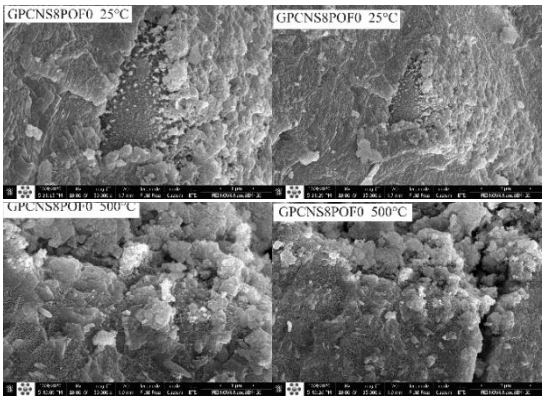

Fig. 13: SEM for GPCNS8POF0 at 25 and 500 °C

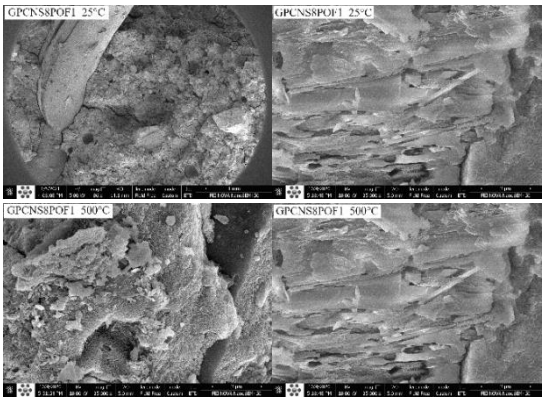

Fig. 14: SEM for GPCNS8POF1at 25 and 500 °C

3.9 Results of XRF Analysis

The results of the analysis of XRF OPCC and GPCs under ASTM C989 [28] standard are shown in Tables 5 and 6. Increasing the temperature up to 500 °C in concrete samples has led to a decrease in the amount of CaO in concrete. This reduction in OPCC is up to 53% and in GPCNS0POF0 to the extent of 31% and in GPCNS8POF0 to the extent of 0.5 % it is arrived. Also, increasing the temperature up to 500 degrees in concrete samples has led to a decrease in the amount of SiO_2 in concrete. This reduction in OPCC reached 41% and in GPCNS0POF0 to 85% and in GPCNS8POF0 to 1% is. It is evident in these tables that the content of elements SiO_2 and CaO in GPCNS0POF0 has decreased by 28% compared to normal concrete. But in design 4, due to the increase of NS, the amount of SiO_2 has increased.

3.10 Results of XRD Analysis

The results of the analysis of XRD OPCC and GPC at temperatures of 25 and 500 °C under the BS EN 13925 standard are shown in Figure 15. The maximum amount of presence of each element in each design is mentioned in each chart. At a temperature of 25 °C, the peak of OPCC samples is more than 3000, and by applying heat of 500 °C to this type of concrete, this peak has reached less than 2000 and has led to the weakening of the properties of OPCC. In GPCs without POFs under the temperature of 25 °C, the peak of the role of the graphs is more than 2000, which has reached less than 2000 after applying the heat of 500 °C. Of course, the presence of more NS in the composition of GPC has been able to improve the conditions of the height of the peaks at 25 °C, and have a smaller drop in the height of the graph peaks of concrete at the temperature of 500 °C. The Appearance Changes of the Cubic and Cylindrical Samples, Before and After Being Exposed to Heating Treatment, are shown in Figure 16.

Table 5: XRF Test Results at 25 °C

Mix Design	SO_3	TiO_2	LOI	Fe_2O_3	Na_2O	K_2O	MgO	CaO	AL_2O_3	SiO_2
OPCC	1.59	0.47	16.4	7.2	1.1	0.91	2.11	37.16	5.63	27.12
GPCNS0POF0	1.16	0.961	16.04	5.64	15.1	1.01	5.05	26.81	8.07	19.57
GPCNS8POF0	2.8	1.17	15.7	3.94	12.87	1.05	3.01	15.2	7.01	36.33

Table 6: XRF Test Results at 500 °C

Mix Design	SO_3	TiO_2	LOI	Fe_2O_3	Na_2O	K_2O	MgO	CaO	AL_2O_3	SiO_2
OPCC	2.41	0.52	16.77	9.85	1.32	1.34	1.95	17.41	9.87	38.25
GPCNS0POF0	2.52	0.74	19.48	7.92	2.1	1.41	2.32	18.41	8.41	36.32
GPCNS8POF0	3.54	0.87	12.95	8.24	4.87	1.5	3.14	15.12	8.21	39.87

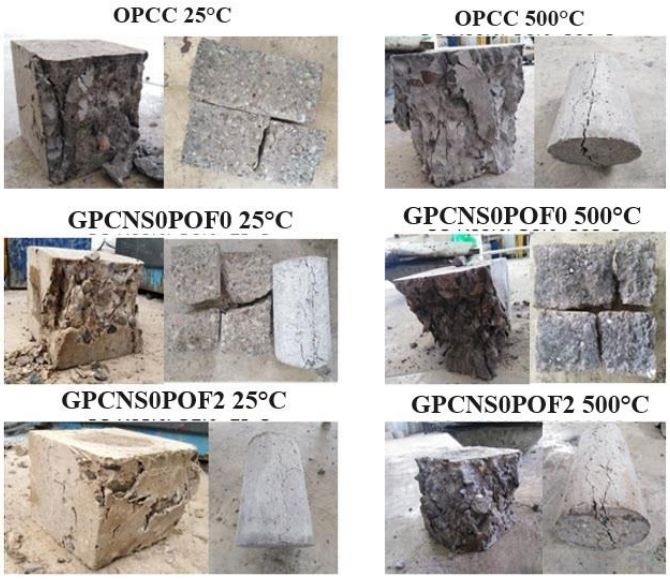

Fig. 16: The Appearance Changes of the Cubic and Cylindrical Samples, Before and After Being Exposed to Heating Treatment

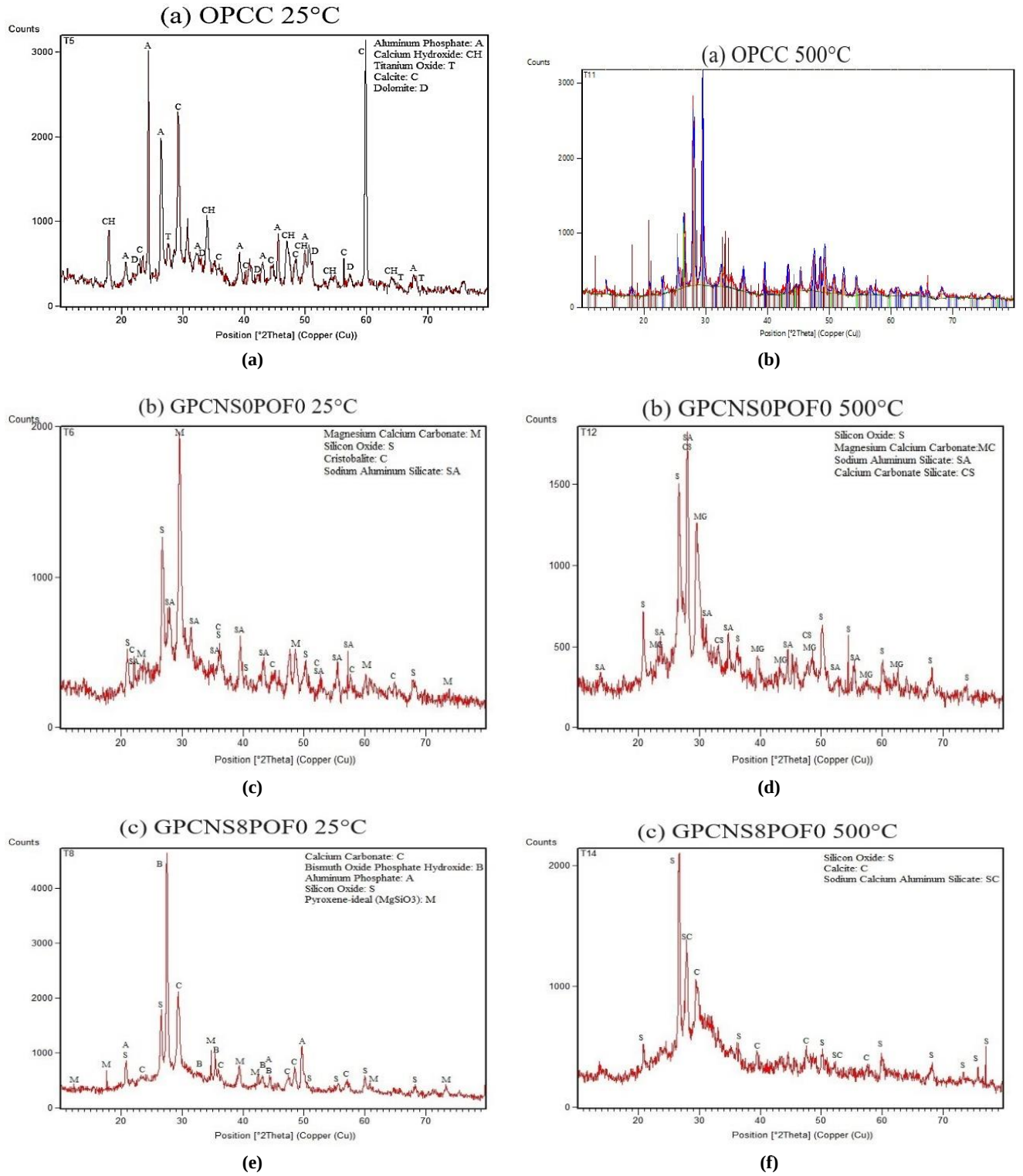

Fig. 15: XRD Patterns for Samples at Different Temperatures. (a) OPCC 25°C ; (b) OPCC 500°C; (c) GPCNS0POF0 25°C; (d) GPCNS0POF0 500°C ; (e) GPCNS8POF0 25°C ; (f) GPCNS8POF0 500°C

4. Conclusions

This study aims to investigate the mechanical and resistance properties against heat in the blast furnace slag-based GPC containing POFs (0-2%) and NS (0-8%). After analyzing the obtained results, it is revealed that NS addition improves the mechanical properties in the GPC samples exposed to heating treatment. POFs addition had a substantial effect on the tensile strength and impact resistance. The results are elaborately provided as follows:

1. The NS addition to the GPC increases the compressive strength from 68 to 82 MPa by 20%. In addition, the

resistance loss level decreases the resistance due to the heating treatment from 16.4 to 8.4%.

2. Regarding the tensile strength, fiber addition improved the tensile strength between 4% and 8% and decreased the loss level due to the heating treatment from 21 to 13% in concrete samples. Moreover, it is revealed that the addition of NS ranging from 4 to 8% to the GPC mixture under the exposure of heating treatment decreased the tensile strength from 21 to 14.5 and 13% of loss, respectively.

3. By conducting a modulus of elasticity test on the concrete, it is realized that the addition of POFs and NS particles to the GPC increases the modulus of elasticity level. Compared to the alkali activated slag concrete, it has greater enhancement in the concrete's modulus of elasticity. Accordingly, adding 8% NS decreases the modulus loss due to heating treatment from 42 to 33%.

4. The resistance test against the drop weight hammer indicates the substantial effect of POFs on the number of impacts in the concrete samples until the appearance of the initial cracks and their complete failure. Besides, the concrete samples exposed to the temperature of 300 °C had experienced subtle changes in the initial crack creation energy and the complete spalling. However, as the temperature increases to 600 °C, it can be observed an intense loss in the initial crack and spalling in the concrete samples.

5. The results of the test UPV for concrete under 25 °C temperature showed that the addition of 8% NS to GPC leads to an improvement in the quality of concrete and an increase in the speed of waves. It is ultrasonic. OPCC under 500 °C heat showed better results than GPC in UPV test results.

6. The results of the analysis SEM, XRF, and XRD were in harmony with other results in this research.

References

[1] Nshimiyimana P, Miraucourt D, Messan A, Courard L. (2009) Calcium carbide residue and rice husk ash for improving the compressive strength of compressed earth blocks. MRS Advances. 2018;3(34-35): -14. https://doi.org/10.1557/adv.2018.147

[2] Ukritnukun S, Sorrell CC, Gregg D, Vance ER, Koshy P. (2018) Potential Use of Ambient-Cured Geopolymers for Intermediate Level Nuclear Waste Storage. MRS Advances.;3(20):1123-31. https://doi.org/10.1557/adv.2018.276

[3] Ghafoor MT, Fujiyama C, Maekawa K. (2021) Mix Design Processing for Self-Compacting Geopolymer Mortar. Journal of Advanced Concrete Technology.19(11):1133-47. https://doi.org/10.3151/jact.19.1133

[4] McNulty E. (2009) Geopolymers: an environmental alternative to carbon dioxide producing ordinary Portland cement. Department of Chemistry, The Catholic University of America.

[5] Radhakrishna. (2020) Strength Assessment in Portland Cement and Geopolymer Composites with Abrams' Law as Basis. JOURNAL OF ADVANCED CONCRETE TECHNOLOGY.;18(6):320-7.

[6] Comrie DC, Kriven WM, editors. (2004) Composite cold ceramic geopolymer in a refractory application. Advances in Ceramic Matrix Composites IX, Proceedings.

[7] Bakharev T. (2006) Thermal behaviour of geopolymers prepared using class F fly ash and elevated temperature curing. Cement and concrete Research;36(6):1134-47. https://doi.org/10.1016/j.cemconres.2006.03.022

[8] Özcan A, Karakoç MB. (2019) The resistance of blast furnace slag-and ferrochrome slag-based geopolymer concrete against acid attack. International Journal of Civil Engineering;17(10):1571-83. https://doi.org/10.1007/s40999-019-00425-2

[9] Mayta-Ponce D, Soto-Cruz P, Huamán-Mamani F. (2019) Thermomechanical evaluation of new geopolymer binder from demolition waste and ignimbrite slits for application in the construction industry. MRS Advances ;4(54):2951-8. https://doi.org/10.1557/adv.2019.474

[10] Kong DL, Sanjayan JG. (2010) Effect of elevated temperatures on geopolymer paste, mortar and concrete. Cement and concrete research.;40(2):334-9. https://doi.org/10.1016/j.cemconres.2009.10.017

[11] Chinapaiya B, Parshwanath RN, Radhakrishnan J, Thirunavukkarasu R. (2020) Adhesive Bond Strength of Steel Bars Embedded in Fly Ash-GGBS-based Geopolymer Concrete. Journal of Advanced Concrete Technology.;18(11):716-29. https://doi.org/10.3151/jact.18.716

[12] Aslani F. (2016) Thermal performance modeling of geopolymer concrete. Journal of Materials in Civil Engineering.;28(1):04015062. https://doi.org/10.1061/(ASCE)MT.1943-5533.0001291

[13] Ganesh AC, Muthukannan M. (2019) Effect of elevated temperature over geopolymer concrete. International Journal of Engineering and Advanced Technology (IJEAT).;9(1S4):450-3. https://doi.org/10.35940/ijeat.A1025.1291S419

[14] Assaedi H, Alomayri T, Shaikh F, Low I-M. (2019) Influence of nano silica particles on durability of flax fabric reinforced geopolymer composites. Materials.;12(9):1459. https://doi.org/10.3390/ma12091459

[15] Deb PS, Sarker PK, Barbhuiya S. (2015) Effects of nano-silica on the strength development of geopolymer cured at room temperature. Construction and building materials.;101:675-83. https://doi.org/10.1016/j.conbuildmat.2015.10.044.

[16] Adak. (2017) Structural performance of nano-silica modified fly-ash based geopolymer concrete. Construction and Building Materials.;135:430-9. https://doi.org/10.1016/j.conbuildmat.2016.12.111.

[17] Ekinci E, Türkmen İ, Kantarci F, Karakoç MB. (2019) The improvement of mechanical, physical and durability characteristics of volcanic tuff based geopolymer concrete by using nano silica, micro silica and Styrene-Butadiene Latex additives at different ratios. Construction and Building

Materials.;201:257-67. https://doi.org/10.1016/j.conbuildmat.2018.12.204.

[18] Adak. (2014) Effect of nano-silica on strength and durability of fly ash based geopolymer mortar. Construction and Building Materials.;70:453-9. https://doi.org/10.1016/j.conbuildmat.2014.07.093.

[19] VU CM, LE TA, SATOMI T, TAKAHASHI H. (2017) Study on effect of chemical composition of geopolymer to improve sludge by using fiber materials. Advanced Experimental Mechanics.;2:168-73. https://doi.org/10.11395/aem.2.0_168

[20] Alberti MG, Enfedaque A, Gálvez JC. (2015) Improving the reinforcement of polyolefin fiber reinforced concrete for infrastructure applications. Fibers.;3(4):504-22. https://doi.org/10.3390/fib3040504.

[21] Ganesh C, Muthukannan M, Kumar AS, Arunkumar K. (2021) Influence of Bacterial Strain Combination in Hybrid Fiber Reinforced Geopolymer Concrete subjected to Heavy and Very Heavy Traffic Condition. Journal of Advanced Concrete Technology.;19(4):359-69. https://doi.org/10.3151/jact.19.359

[22] Yousefvand M, Sharifi Y, Yousefvand S. (2019) An Analysis of the Shear Strength and Rupture Modulus of Polyolefin-Fiber Reinforced Concrete at Different Temperatures. Journal of civil Engineering and Materials Application.;3(4):238-54. https://doi.org/ 10.22034/jcema.2019.102829

[23] Rashad AM. (2019) The effect of polypropylene, polyvinyl-alcohol, carbon and glass fibres on geopolymers properties. Materials Science and Technology.;35(2):127-46. https://doi.org/10.1080/02670836.2018.1514096.

[24] Nagajothi S, Elavenil S. (2021) Shear Prediction of geopolymer concrete beams using Basalt/Glass FRP bars. Journal of Advanced Concrete Technology.;19(3):216-25. https://doi.org/10.3151/jact.19.216

[25] Adhikary SK, Rudzionis Z, Balakrishnan A, Jayakumar V. (2019) Investigation on the mechanical properties and post-cracking behavior of polyolefin fiber reinforced concrete. Fibers.;7(1):8. https://doi.org/10.3390/fib7010008

[26] Noushini A, Castel A, Gilbert RI. (2019) Creep and shrinkage of synthetic fibre-reinforced geopolymer concrete. Magazine of Concrete Research.;71(20):1070-82. https://doi.org/10.1680/jmacr.18.00053.

[27] Pilehvar S, Cao VD, Szczotok AM, Carmona M, Valentini L, Lanzón M, et al. (2018) Physical and mechanical properties of fly ash and slag geopolymer concrete containing different types of micro-encapsulated phase change materials. Construction and Building Materials.;173:28-39. https://doi.org/10.1016/j.conbuildmat.2018.04.016

[28] C989/C989M-18a (2018) A. Standard specification for slag cement for use in concrete and mortars. ASTM International West Conshohocken, PA.

[29] EN B. (2000) Testing hardened concrete. Method of determination of compressive strength of concrete cubes. BS EN 12390 Part.;3.

[30] ASTM C-. Standard Test Method for Splitting Tensile Strength of Cylindrical Concrete Specimens.

[31] Galan A, (1967) editor Estimate of concrete strength by ultrasonic pulse velocity and damping constant. Journal Proceedings.

[32] 544-2R-89 A. (1999) 'Measurement of properties of fiber reinforced concrete'. Reported by ACI Committee.;544.

[33] Bakhtiyari S, Allahverdi A, Rais-Ghasemi M, Zarrabi B, Parhizkar T. (2011) Self-compacting concrete containing different powders at elevated temperatures–Mechanical properties and changes in the phase composition of the paste. Thermochimica acta.;514(1-2):74-81. https://doi.org/10.1016/j.tca.2010.12.007

[34] Bentz DP. (2000) Fibers, percolation, and spalling of high-performance concrete. Materials Journal.;97(3):351-9.

[35] Zhang B, Bicanic N. (2002) Residual fracture toughness of normal-and high-strength gravel concrete after heating to 600 C. Materials Journal.;99(3):217-26.

[36] 363 AC, (1984) editor State-of-the-art Report on High-strength Concrete (ACI 363R-84): American Concrete Institute.

[37] Nath P, Sarker PK. (2017) Flexural strength and elastic modulus of ambient-cured blended low-calcium fly ash geopolymer concrete. Construction and Building Materials.;130:22-31. https://doi.org/10.1016/j.conbuildmat.2016.11.034.

[38] Diaz-Loya EI, Allouche EN, Vaidya S. (2011) Mechanical properties of fly-ash-based geopolymer concrete. ACI materials journal.;108(3):300.

[39] 363 AC. (1993) State of the art of high strength concrete. American Concrete Institute.

[40] Sumajouw D, Hardjito D, Wallah S, Rangan B. (2007) Fly ash-based geopolymer concrete: study of slender reinforced columns. Journal of materials science.;42(9):3124-30. https://doi.org/10.1007/s10853-006-0523-8.

[41] Sahmaran M, Yurtseven A, Yaman IO. (2005) Workability of hybrid fiber reinforced self-compacting concrete. Building and Environment.;40(12):1672-7. https://doi.org/10.1016/j.buildenv.2004.12.014.

[42] Whitehurst EA, (1951) editor Soniscope tests concrete structures. Journal Proceedings.

[43] Kwan WH, Ramli M, Kam KJ, Sulieman MZ. (2012) Influence of the amount of recycled coarse aggregate in concrete design and durability properties. Construction and Building Materials.;26(1):565-73. https://doi.org/10.1016/j.conbuildmat.2011.06.059.

[44] Ren W, Xu J, Bai E. (2015) Strength and ultrasonic characteristics of alkali-activated fly ash-slag geopolymer concrete after exposure to elevated temperatures. Journal of Materials in Civil Engineering.;28(2):04015124. https://doi.org/10.1061/(ASCE)MT.1943-5533.0001406.

[45] Fan F, Liu Z, Xu G, Peng H, Cai C. (2018) Mechanical and thermal properties of fly ash based geopolymers. Construction and Building Materials.;160:66-81. https://doi.org/10.1016/j.conbuildmat.2017.11.023

[46] Olivito R, Zuccarello F. (2010) An experimental study on the tensile strength of steel fiber reinforced concrete. Composites Part B: Engineering.;41(3):246-55. https://doi.org/10.1016/j.compositesb.2009.12.003.

[47] Du H, Du S, Liu X. (2014) Durability performances of concrete with nano-silica. Construction and building materials.;73:705-12.https://doi.org/10.1016/j.conbuildmat.2014.10.014.

[48] Hua S, Zhang L, Zhang J, Jiang M, Guo D, Tong F, et al. (2020) Study on Physical and Chemical Properties of High Magnesium Nickel Slag-Phosphogysum Composite Cementitious Materials in Different Particle Sizes. Journal of Advanced Concrete Technology.;18(3):129-38. https://doi.org/10.3151/jact.18.129